Heliyon 6 (2020) e05187

Contents lists available at ScienceDirect

Heliyon

journal homepage: www.cell.com/heliyon

Research article

Synthesis, density functional theory (DFT) studies and urease inhibition activity of chiral benzimidazoles

Hasil Aman [a,b,*], Naghmana Rashid [a], Zaman Ashraf [a], Aamna Bibi [b], Hsin-Tsung Chen [b], Nadaraj Sathishkumar [b]

[a] Department of Chemistry, Faculty of Science, Alama Iqbal Open University, Islamabad 44000, Pakistan
[b] Department of Chemistry, School of Science, Chung Yuan Christian University, Taoyuan 32023, Taiwan

ARTICLE INFO

Keywords:
Organic chemistry
Pharmaceutical chemistry
Theoretical chemistry
Benzimidazole
Urease inhibition
Density functional theory
HOMO
LUMO
Molecular docking

ABSTRACT

A variety of benzimidazole by the heterocyclization of orthophenylenediamine were synthesized in 69–86% yields. The synthesized compounds **3a-f** and **6a-f** were characterized and further investigated as jack bean urease inhibitors. Density functional theory (DFT) studies were performed utilizing the basis set B3LYP/6-31G (d, p) to acquire perception into their structural properties. Frontier molecular orbital (FMO) analysis of all compounds 3a–f and 6a-f was computed at the same level of theory to get a notion about their chemical reactivity and stability. The mapping of the molecular electrostatic potential (MEP) over the entire stabilized molecular geometry indicated the reactive centers. They exhibited urease inhibition activity with IC50 between 22 and 99 μM. Compounds containing withdrawing groups on the benzene ring (**3d, 6d**) were not showing significant urease inhibition. The value obtained for **3a, 3b, 3f** had shown their significant urease inhibition for both theoretical and experimental. Notably, the compound having S-configuration (**3a**) (22.26 ± 6.2 μM) was good as compared to its R enantiomer **3f** (31.42 ± 23.3 μM). Despite this, we elaborated the computational studies of the corresponding compounds, to highlight electronic effect which include HOMO, LUMO, Molecular electrostatic potential (MEP) and molecular docking.

1. Introduction

Benzimidazoles are well known nitrogen-containing bioactive compounds. They showed a variety of activities including anti-diabetic [1], antimicrobial [2], antifungal [3], antiviral [4], anti-cancer activity [5a,b] and anthelminthic [6]. Recent studies in medicinal chemistry have demonstrated them as potential drug motifs for the pharmaceutical industry [7]. They have also well-known applications in chemo-sensing [8], fluorescence [9], crystal engineering [10], corrosion science [11a, b] and asymmetric catalysis [12]. The bioactivity of drug molecule depends predominantly on their interaction with drug targets, such as proteins, enzymes, nucleic acids and the biological membranes [13a,b]. The efficacy and of the imidazole can be impute to its H-bond donor and acceptor ability as well as its binding affinity with metals [14] (see Figure 1).

Urease enzymes belongs to a class of hetero-polymeric enzymes. It is found in excess quantities in beans like soya beans, jack beans, and some other plant seeds [15]. The active site of urease comprises of two nickel(II) atoms (Ni^{+2}) [16]. Urease converts urea into NH_3 and carbon dioxide by hydrolysis [17a,b]. It has been reported that ureases are responsible for pathogenicity such as stomach cancer, peptic ulceration, hepatic coma and urinary stones [18]. Besides in agriculture, high urease activity results in serious environmental and commercial losses by releasing abnormally enormous amounts of NH_3 in atmosphere [19a,b]. The detailed mechanism of urease suggested that the nickel atoms are playing key role in their activity [20].

Different compounds have been studied for their urease inhibition response [21]. However, benzimidazoles as jackbean urease inhibitors and their DFT studies have rarely ever found in the literature. In this context, some chiral derivatives of benzimidazoles of benzimidazoles were synthesized, several quantum chemical descriptors in order to interpret various molecular properties such as electronic structure, stability, reactivity, in the interest of determining how they could have an impact on our understanding of the experimental observations and describing various aspects of chemical binding. Finally, they have been

* Corresponding author.
E-mail address: hasilaman786@gmail.com (H. Aman).

https://doi.org/10.1016/j.heliyon.2020.e05187
Received 13 May 2020; Received in revised form 2 August 2020; Accepted 5 October 2020

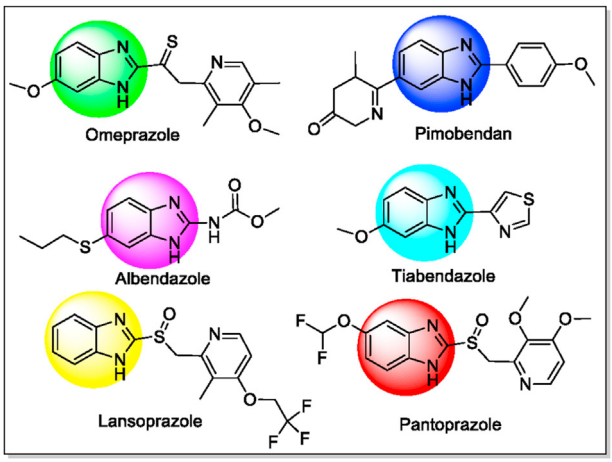

Figure 1. Biologically active drug molecules containing benzimidazoles like omeprazole (used for gastroesophageal diseases), pimobendan (vasodilator), albendazole (parasitic worm infestations), tibendazole, (antifungal agent), lansoprazole (Anti acid) and pantoprazole (proton pump inhibitor) [1, 2, 3, 4, 5, 6, 7].

tested for their Jack Bean Urease inhibition activity. The comparative inhibitory activity of the most potent enantiomer was also calculated.

2. Experimental

2.1. General

All chemicals for the synthesis of chiral benzimidazole derivatives (**3a-f** and **6a-f**) and Jack Bean Urease were purchased from Sigma Co. Büchi melting point B-540 was used for measurement of melting points while Nicolet iS10 spectrophotometer was used for IR spectra. The NMRs of all compounds were run on an Advance 400 MHz NMR spectrometer in DMSO and $CDCl_3$ solutions. EIMS were recorded on JEOL MSR mass spectrometer.

2.2. Synthesis

2.2.1. General procedure for synthesis of 3a~f

Equimolar amount (0.0073mol) of o-phenylenediamine (different derivatives) and L-lactic acid were taken in 4N HCl (30.0 ml) and refluxed for 6 h. Whereas, reaction was monitored by thin layer chromatography. Reaction mixture was filtered and neutralized by liquid ammonia (NH_4OH) to get solid product, which is then purified by flash column using 8:2 of eluents n-hexane and ethyl acetate.

2.2.2. General procedure for synthesis of 6a~f

Naproxenoyl chloride (**4a-f**) was prepared according to given procedure [22]: 5.0 ml of $POCl_3$ was added to a solution of 0.01 mol naproxen in 30 ml of *m*-xylene. The reaction mixture was refluxed for 3 h, the settled down and cooled precipitates were filtered off, washed by ether, and on drying gave a colorless crystal (mp 81 °C). Obtained Yield 73 %; ^{1}H NMR: δ ppm = 1.62 (d, 3H, J = 6.6 Hz, CH_3), 3.84 (q, 1H, J = 6.5, CH), 3.93 (s, 3H, OCH_3), 7.12–7.74 (m, 6H, Ar). ^{13}CNMR; 17.53 (CH_3), 46.31(CH), 54.45 (OCH_3), 106.30, 119.00, 126.13, 126.30, 127.11, 129.01, 129.61, 134.04, 135.20, 157.70, 179.31.

Equimolar quantity of naproxenoyl chloride (**4a-f**) (0.0073 mol) and orthophenylenediame (different derivatives) were taken in 4N HCl (60 ml) were heated underneath reflux for 6 h. Reaction mixture was filtered off and neutralized with NH_4OH to induce the solid compound, which is then purified by silica gel column.

2.2.3. General procedure for separation of enantiomers 3a, 3f and 6a, 6f

Desired chiral benzimidazole was dissolved (10 mg/L) in the solvent system of the mobile phase (n-hexane: iso-propanol, 95/5). Each sample (20 μl) was then injected into HPLC with the mobile phase including the reverse phase (CH_3CN/H_2O) and normal phase (n-hexane/isopropanol). HPLC system comprised of two pumps (an intelligent pump L-200, L-6000 pump), UV-Vis detector L-4200 and an integration system. The chiral stationary phase was LiChroCART 250-4 (S,S)-Whelk-O1 (5 mm) and LiChroCART 250-4 (R,R)-Whelk-O1 (5mm) with (3R,4R)-and (3S,4S)-4-(3,5-dinitrobenzamido)-1,2,3, 4-tetrahydro-phenanthrene as packing materials. The wavelength used for UV-Vis was set at 210 nm while the chromatography was done at room temperature. To separate the racemate, the samples were injected hundreds of times under a given condition. The pure enantiomer was collected, concentrated under a vacuum evaporator to dry and stored [23].

2.2.4. General procedure for urease inhibition studies [24].

The urease inhibitory activity of synthesized chiral benzimidazoles **3a-f** and **4a-b** was determined by measuring the amount of ammonia produced by the indophenols method described by Weather burn. The reaction mixtures, comprising 20 μL of enzyme (Jack bean urease, 5 U/mL) and 20 μLof test compounds in 50 lL buffer (100 micro molar urea, 0.01 MK_2HPO_4, 1 micro molar EDTA and 0.01 M Lithium dichloride, pH 8.15), were incubated for 10 min, at 37 °C in 96-well plate. Briefly, 40 μL each of phenol reagents (1%, w/v phenol and 0.005%, w/v sodium nitroprusside) and 70 μL of alkali reagent (0.5%, weight by volume NaOH and 0.1% active chloride, sodium hypochloride) were added to each well. The absorbance at 625.0 nm was measured after 30.0 min, using a microplate reader (OPTI Max, Tunable). All these reactions were performed in atriplicate. The urease inhibition activities were calculated according to the following formula:

$$\text{Urease inhibition activity } (\%) = (OD_{control} - OD_{sample} \times 100)/OD_{control}$$

Where $OD_{control}$ and OD_{sample} represents the optical densities in the absence and presence of sample respectively. Thiourea was used as the standard inhibitor for urease inhibition.

2.3. Characterization

2.3.1. (R or S)-1-(1H-benzo[d] imidazol-2-yl)ethanol (3a and 3f)

(85%), m.p 182 °C, Rf: 0.4 (n hexane: ethyl acetate) 3:1; IR: ν: 2942 (=C–H), 2843 (-CH_3), 1615 (C=N), 3500 (O–H), 3305(N–H). ^{1}HNMR (400 MHz, $CDCl_3$) δ ppm: 1.52 (s, 3H, CH_3, J = 6.8 Hz), 4.96 (q, 1H, J = 6.8), 7.3 (m, 4H, Ar–H), 12.2 (s, 1H, NH); ^{13}CNMR, (75 MHz) δ ppm: 70 (chiral carbon),141.5 (C=N), 138.9, 115. 123 (Ar); HRMS (ESI): m/z calculated for $C_9H_9N_2O$ [M^+]; 163.0871, found 163.0874 (M^+ + H).

2.3.2. (±)-1-(6-chloro-1H-benzo[d] imidazol-2-yl) ethanol (3b)

(80%), m.p 233 °C; IR: ν: 3500 (O–H), 1615 (C=N), 3300 5 (NH), 2952 (CH), 2982 (C-H_{Ar}), 700 (C–Cl). ^{1}H-NMR (400 MHz, $CDCl_3$) δ ppm: 1.49 (d, 3H, CH_3), 1.48–1.50 (d, J = 6.8 Hz), 4.92 (q, 1H, CH) 4.91–4.93(J = 6.8), 7.75 (d, 1H, Ar), range (d, J = 8 Hz), 7.61 (s, 1H, Ar), 7.14 (d, 1H, Ar), 7.13–7.45 (d, J = 8 Hz), 12.2 (s, 1H, NH); ^{13}CNMR, (75 MHz) δ ppm: 70.4 (chiral carbon),143.9 (C=N imidazole), 134.8-112.5 (Ar); HRMS (ESI): m/z calculated for $C_9H_9ClN_2O$ [M^+ + H^+], 197.0482 found 197.0484.

2.3.3. (±)-1-(6-bromo-1H-benzo[d]imidazol-2-yl)ethanol (3c)

(82%), m.p 193 °C; IR: ν: 1615(C=N), 3500 (O–H), 3320(N–H), 1550 (C–Br), 1335 (C–N).^{1}HNMR (400 MHz, $CDCl_3$) δ ppm: 1.52 (d, 3H, CH_3), 1.46–1.63 (d, J = 6.8 Hz), 4.99 (q, 1H, CH) 4.95–5.01 (J = 6.8), 7.66 (d, 2H, Ar), range (s, J = 3.2 Hz),8.08 (d, 2H, Ar), range (d, J = 6.0 Hz), 8.38 (s, 1H, Ar), 12.20 (s, 1H, NH), 3.33 (s, 1H, OH); ^{13}CNMR, (75 MHz) δ ppm: 23.3(CH_3) 69.8 (chiral carbon),143.5 (C=N imidazole), 134.8-

112.5 (Ar); HRMS (ESI): m/z calculated for $C_9H_9BrN_2O$ [$M^+ + Na^+$], 262.9796; found, 262.9799.

2.3.4. (±)-1-(6-nitro-1H-benzo[d] imidazol-2-yl)ethanol (3d)

(78%), m.p 186 °C: IR: v: 1615 (C=N), 3500 (O–H), 3320(N–H), 1550 (N–O), 1335 (C–N). ^{1}HNMR (400 MHz, $CDCl_3$) δ ppm: 1.52 (d, 3H, CH_3), 1.51–1.52 (d, J = 6.8 Hz), 4.99 (q, 1H, CH) 4.97–5.01 (J = 6.8), 7.66 (d, 2H, Ar), range (d, J = 3.2 Hz), 8.08 (d, 2H, Ar–H), range (d, J = 6.0 Hz), 8.38 (s, 1H, Ar–H), 12.20 (s, 1H, NH), 3.33 (s, 1H, OH); ^{13}CNMR, (75 MHz) δ ppm: 69.7 (chiral carbon),142.21 (C=N imidazole), 145.0-110.5 (Ar–H); HRMS (ESI): m/z calculated for $C_9H_9N_3O3$ [$M^+ + NH_4^+$], 225.0988 found 225.0986.

2.3.5. (±)-1-(6-methyl-1H-benzo[d]imidazol-2-yl)ethanol (3e)

(86%), m.p 195 °C; IR: v: 1615 (C=N), 3500 (O–H), 3320 (N–H), 1335 (C–N). ^{1}HNMR (400 MHz, DMSO) δ ppm: 1.51 (d, 3H, CH_3), 1.47–1.49 (d, J = 6.8 Hz), 2.5 (s, 3H, CH_3) 4.99 (q, 1H, CH) 4.85–4.93 (J = 6.8), 7.66 (d, 1H, Ar–H), 8.08 (d, 1H, Ar), 8.38 (s, 1H, Ar–H), 12.20 (s, 1H, NH), 3.33 (s, 1H, O–H); ^{13}CNMR, (75 MHz) δ ppm: 70 (chiral carbon), 141 (C=N imidazole), 138.8, 115.2 (Ar–H), 23.2 MHz (CH_3), 25 (CH_3); HRMS (ESI): m/z calculated for $C_{10}H_{12}N_2O$ [$M^+ + Na^+$], 199.0847; found, 199.0847 ($M^+ + Na^+$).

2.3.6. (S/R)-1-(2-methoxynaphthalen-6-yl)ethyl)-1-H-benzo[d]imidazole (6a and 6f)

(73%), m.p 212 °C; IR: v: 2940 (C=C–H), 1615 (C=N), 3320 (N–H), 1325 (C–O), 2980 (C-H_{Ar}). ^{1}HNMR (400 MHz, $CDCl_3$) δ ppm: 1.76 (d, 3H, CH_3), 1.75–1.78 (d, J = 6.8 Hz), 3.87 (s, 3H, OCH_3), 4.48 (q, 1H, CH) 4.95-4.52 (J = 6.8), 7.70 (d, 2H, Ar), range (d, J = 6.2 Hz), 7.26 (d, 2H, Ar), range (d. J = 6.0 Hz), 7.47 (s, 1H, Ar), 7.57 (d, 1H, Ar), range (d, J = 3.2 Hz), 7.04 (d, 1H, Ar), range (d, J = 3.2 Hz), 7.07 (s, 1H, Ar), 7.38 (d, 1H, Ar); ^{13}CNMR, (75 MHz) δ ppm: 70 (chiral carbon),141.5 (C=N imidazole), 152.2-115.3 (Ar); HRMS (ESI): m/z calculated for $C_{20}H_{18}N_2O$ [$M^+ + H^+$], 303.1497; found, 303.1499.

2.3.7. (±)-6-chloro-2-((R)-1-(2-methoxynaphthalen-6-yl)ethyl)-1H-benzo [d]imidazol (6b)

(70%), m.p 224 °C; IR: v: 2980 (C=C–H), 1615 (C=N), 3500 (O–H), 3320(N–H). ^{1}HNMR (400 MHz, $CDCl_3$) δ ppm: 3.91 (s, 3H, OCH_3), 1.76 (d, 3H, CH_3), 1.56–1.57(d, J = 6.8 Hz), 4.48 (q, 1H, CH) 1.76–1.79(J = 6.8), 7.70 (d, 1H, Ar), range (d, J = 6.2 Hz), 7.26 (d, 1H, Ar–H), range (d, J = 6.0 Hz), 7.47 (s, 1H, Ar–H), 7.57 (d, 1H, Ar–H), range (d, J = 3.2), 7.04 (d, 1H, Ar–H), range (d, J = 3.2 Hz), 7.07 (s, 1H, Ar–H), 7.38 (d, 1H, Ar–H), range (d, J = 2.0 Hz), 7.35 (d, 1H, Ar–H), range (d, J = 2.0 Hz), 12.3 (s, 1H, NH), 7.67 (s, 1H, Ar–H), 3.7 (s, 3H, OCH_3); ^{13}CNMR, (75 MHz) δ ppm: 70MHz (chiral carbon),141.5 (C=N imidazole), 156.2, 105.4 (Ar–H), 130.3 (C–Cl). HRMS (ESI): m/z calculated for $C_{20}H_{17}ClN_2O$ [$M^+ + H^+$], 337.1108; found, 337.1109.

2.3.8. (±)-6-bromo-2-((R)-1-(2-methoxynaphthalen-6-yl)ethyl)-1H-benzo [d]imidazol (6c)

(69%), m.p 202 °C; IR: v: 2976 (C=C–H), 1614 (C=N), 3500 (O–H), 3323(N–H). ^{1}HNMR (400 MHz, DMSO) δ ppm: 1.71 (d, 3H, CH_3), 1.55–1.56(d, J = 6.7 Hz), 3.90 (s, 3H, OCH_3), 4.48 (q, 1H, CH) 1.75–1.78(J = 6.7), 7.70 (d, 1H, Ar–H), range (d, J = 6.2 Hz), 7.16 (d, 1H, Ar), range (d, J = 6.0 Hz), 7.32 (s, 1H, Ar), 7.35 (d, 1H, Ar), range (d, J = 3.2), 7.01 (d, 1H, Ar), range (d, J = 3.2 Hz), 7.01 (s, 1H, Ar), 7.29 (d, 1H, Ar), range (d, J = 2.0 Hz), 7.26 (d, 1H, Ar), range (d, J = 2.0 Hz), 12.3 (s, 1H, NH), 7.67 (s, 1H, Ar), 3.3 (s, 3H, OCH_3); ^{13}CNMR, (75 MHz) δ ppm: 70MHz (chiral carbon),140.1 (C=N imidazole), 153.2, 105.4 (Ar), 117.5 (C–Br). HRMS (ESI): m/z calculated for $C_{20}H_{17}BrN_2O$ [$M^+ + H^+$], 381.0603; found, 381.0605.

2.3.9. (±)-6-Nitro-2-((R)-1-(2-methoxynaphthalen-6-yl)ethyl)-1H-benzo [d]imidazol (6d)

(69%), m.p 210 °C; IR: v: 2988 (C=C–H), 1612 (C=N), 3500 (O–H), 3331(N–H). ^{1}HNMR (400 MHz, $CDCl_3$) δ ppm: 3.91 (s, 3H, OCH_3), 1.69 (d, 3H, CH_3), 1.55–1.56(d, J = 6.7 Hz), 4.38 (q, 1H, CH) 1.75–1.78(J = 6.7), 7.70 (d, 1H, Ar), range (d, J = 6.2 Hz), 7.16 (d, 1H, Ar), range (d, J = 6.0 Hz), 7.32 (s, 1H, Ar), 7.35 (d, 1H, Ar), range (d, J = 3.2), 7.01 (d, 1H, Ar), range (d, J = 3.2 Hz), 7.01 (s, 1H, Ar), 7.29 (d, 1H, Ar), range (d, J = 2.0 Hz), 7.26 (d, 1H, Ar), range (d, J = 2.0 Hz), 12.3 (s, 1H, NH), 7.67 (s, 1H, Ar), 3.31 (s, 3H, OCH_3); ^{13}CNMR, (75 MHz) δ ppm: 70 (chiral carbon),141.1 MHz (C=N imidazole), 154.6, 105.4 (Ar), 144.5 (C–NO_2). HRMS (ESI): m/z calculated for $C_{20}H_{17}N_3O_3$ [$M^+ + Na^+$], 370.1168; found, 370.1165.

2.3.10. (±)-6-methyl-2-((R)-1-(2-methoxynaphthalen-6-yl)ethyl)-1H-benzo[d] imidazol (6e)

(69%), m.p 212 °C; IR: v: 2988 (C=C–H), 1612 (C=N), 3500 (O–H), 3331(N–H). ^{1}HNMR (400 MHz, $CDCl_3$) δ ppm: 1.69 (d, 3H, CH_3), 1.55–1.56(d, J = 6.5 Hz), 3.91 (s, 3H, OCH_3), 4.38 (q, 1H, CH) 1.75–1.78(J = 6.6), 7.71 (d, 1H, Ar), range (d, J = 6.2 Hz), 7.16 (d, 1H, Ar), range (d, J = 6.1 Hz), 7.32 (s, 1H, Ar), 7.35 (d, 1H, Ar), range (d, J = 3.2), 7.01 (d, 1H, Ar), range (d, J = 3.2 Hz), 7.01 (s, 1H, Ar), 7.29 (d, 1H, Ar), range (d, J = 2.0 Hz), 7.26 (d, 1H, Ar), range (d, J = 2.0 Hz), 12.3 (s, 1H, NH), 7.67 (s, 1H, Ar), 3.31 (s, 3H, OCH_3); ^{13}CNMR, (75 MHz) δ ppm: 70 (chiral carbon),141.6 (C=N imidazole), 152.6, 105.4 (Ar), 22.6 (C–CH_3). HRMS (ESI): m/z calculated for $C_{21}H_{20}N_2O$ [$M^+ + H^+$], 317.1654; found, 317.1650.

3. Results and discussions

Numerous synthetic routes have been used for the preparation of benzimidazoles however our recent investigations involving hetrocyclization of orthophenylenediammine are very encouraging [25a,b,c]. Thus in our initial attempt we have synthesized the chiral derivatives of benzimidazole by the hetrocyclization of orthophenylenediammine with

Table 1. Synthesis and urease inhibition studies of benzimidazoles derivatives **3a-3f**.

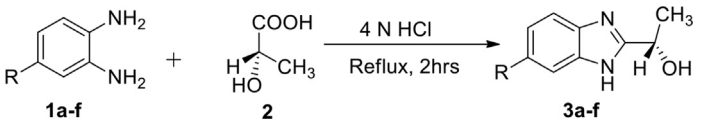

1a-f 2 3a-f

compound	R	% yield	IC50 ± SEM (μM)
3a	H (R config.)	85	22 ± 6.2
3b	Cl	80	38 ± 18.2
3c	Br	82	46 ± 8.3
3d	NO_2	78	66 ± 27.4
3e	CH_3	86	36 ± 9.2
3f	H (S-config.)	85	31 ± 23.3

Table 2. Synthesis and urease inhibition studies of benzimidazoles derivatives **6a-6f**.

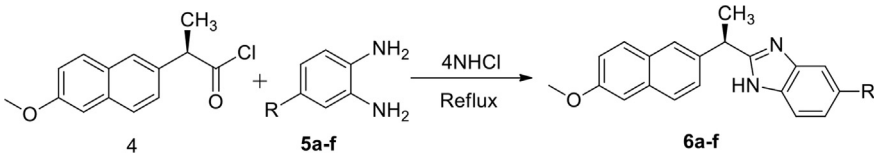

compound	R	% yield	IC50 ± SEM (μM)
6a	H (R config)	73	38 ± 1.3
6b	Cl	70	36 ± 1.7
6c	Br	69	51 ± 9.3
6d	NO_2	69	99 ± 9.4
6e	CH_3	69	44 ± 2.4
6f	H (S-config.)	73	39 ± 2.4

lactic acid and secondly, evaluate their urease inhibition studies (see Tables 1 and 2).

Chiral benzimidazoles were obtained in a yield range 70–86%. The FT-IR spectrum displayed several characteristic bands round about 3305.08, 3152.47 2982.12, 2952.46, 1605, and 1145 cm^{-1}. More importantly the presence of characteristic peak C=N at 1605-1620 cm^{-1} has provided a strong evidence of formation imidazole ring of benzimidazole [26a,b,c]. While the remaining observed vibration bands were assigned to (NH) stretching (3305.08), (Ar–H) stretching vibrations (2982.12), (CH) stretching vibrations (2952.46), (C=N) stretching vibration (1605) and (OH) stretching vibration (3400cm^{-1}) [27a,b,c].

In the ^{1}H NMR and ^{13}CNMR we have found the characteristic peaks of benzimidazoles (Figure S4 to S7 supporting information). The most downfield signal around 12.2 ppm for NH, methyl group at 1.51 ppm as a doublet due to 'AB' spin system coupling with one neighboring proton, the peaks of aromatic ring ranging from 7.10-7.42 ppm. The molecular masses of the synthesized compounds were determined by their EIMS.

3.1. DFT studies

3.1.1. Geometry optimization

Currently, computational methods attract a lot of attention to the study of the SAR of compounds, and DFT study is one of the most prominent calculation approach due to its accuracy and less time duration. The energy and geometries of **3a-f** (Figure 2) and **6a-f** (Fig. S1) were optimized at the B3LYP/6-31G (d, p) level of DFT by Gaussian 09 program [28a,b,c]. In addition, investigation like MEP and FMOs carried out on optimized geometries [29].

3.1.2. Frontier molecular orbital (FMO) analysis

This method is widely employed to explain the electronic as well as the optical properties of compounds. The main participants during molecular interactions, are the highest occupied molecular orbital (HOMO) and the lowest unoccupied molecular orbital (LUMO). These values used to determine the kinetic stability and chemical reactivity of molecules. The energy of LUMO energy level represents electron-accepting abilities while HOMO shows electron donating ability.

We depict the HOMO-LUMO energy diagram (Fig. S2 and Fig. S3) show that electron rich region (red), electron scale region (green). The populations analysis revealed that iso-densities are mainly concentrated on imidazole and aromatic moieties. The HOMO-LUMO energy gaps are summarized in Table 3. This energy gap for **3a, 3f** is found to be the maximum and equal to 5.61 eV, while the least band gap (4.48 eV and 3.71 eV,) was determined for **3d, 6d**. The iso-density in HOMO of **3a, 3f** is mainly spread only to the rings, which reflects less conjugation. This observation indicates that the HOMO-LUMO gap in **3a, 3f** should display the highest energy among all products studied, and indeed this was the case.

In **3e**, the density on the HOMO spread over the entire scaffold (including the CH_3 substituent) in the same region as compared to **3a, 3f**; therefore, its energy gap is comparable to that of **3a, 3f** (i.e., of 5.51 eV). This slightly smaller energy gap in **3e** is expected due to the presence of

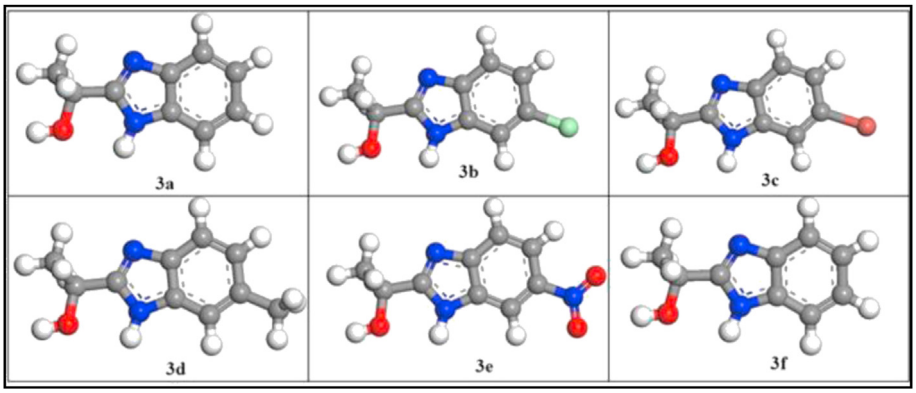

Figure 2. Optimized structures of compounds **3a-f** at B3LYP/6-31G (d, p); Atom color code: green, chlorine; red, oxygen; gray, carbon; brown, bromine blue, nitrogen; white, hydrogen.

Table 3. HOMO and LUMO energies along with HOMO-LUMO energy gap of products **3a-f** and **6a-f**.

Entry	HOMO (a.u)	LUMO (a.u)	HOMO/LUMO (*ΔE/Ev*)
3a	-0.21439	-0.00815	5.61
3b	-0.21869	-0.02077	5.38
3c	-0.21706	-0.02119	5.33
3d	-0.24394	-0.07919	4.48
3e	-0.20726	-0.00459	5.51
3f	-0.21438	-0.00814	5.61
6a	-0.20685	-0.04243	4.47
6b	-0.20979	-0.04580	4.55
6c	-0.20984	-0.04580	4.46
6d	-0.21473	-0.07855	3.71
6e	-0.20505	-0.04174	4.44
6f	-0.20663	-0.04241	4.47

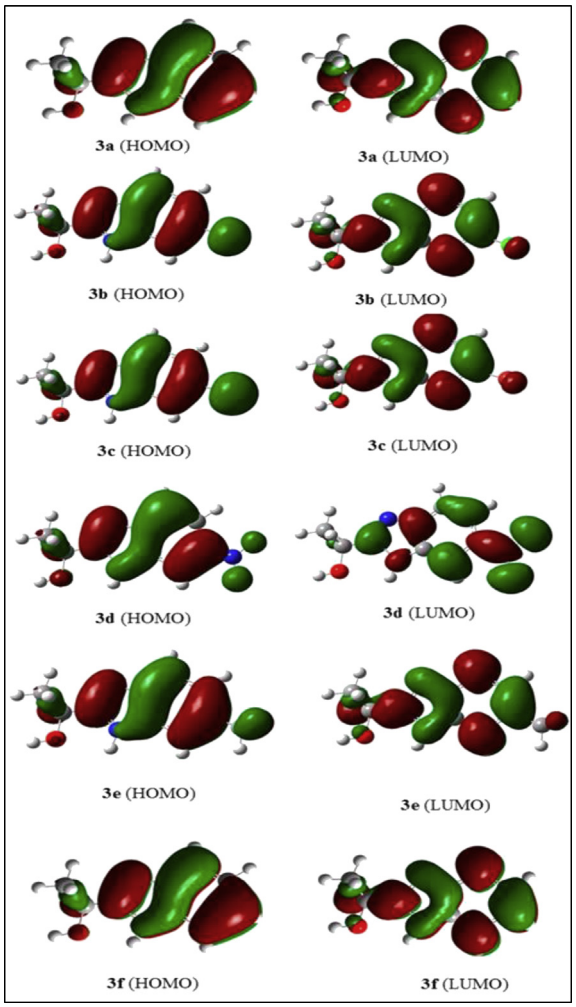

Figure 3. Frontier molecular orbitals (HOMO-LUMO) of compounds **3a-f** at B3LYP/6-31G (d, p) base set level. (FMO for **6a-f** are included in figure S2).

planarity and the electron donating-effect of the methyl group (see Figure 3).

3.1.3. Molecular electrostatic potential (MEP)

$$V(r) = \sum \frac{Z_A}{|R_A - r|} - \int \frac{\rho(r')}{|r' - r|} dr' \quad (1)$$

Z_A is the nuclear charge present at a distance R_A and ρ(r') representing electron density. The molecular electrostatic potential (MEP) mapping utilize DFT techniques can be beneficial in biochemistry to decide drug-receptor interactions. The MEP is associated chemically active sites of a molecule and additionally improves the perception of molecular reactivity, electrophilic reactions, substituent effects, inter and intra-molecular relations. The increasing electrostatic potential in the following order: red, yellow, blue and green. According to color scale, electron rich (red), slightly electron rich (yellow) which is due to the lone pair of oxygen atom, electron deficient (blue) region of the molecule was surrounded over the hydrogen atoms. Which is due to the electronegative nitrogen atom being attached with the hydrogen atoms. The neutral electrostatic potential (green) envelopes over the π-system of the ring. The electrophilic region of the molecule was predicted around the hydrogen atoms of benzene and imidazole ring. The reactive sites of electrophilic and nucleophilic attacks are investigated for all products **3a~f, 6a~f** was computed by MEP the use of B3LYP/6-31G (d, p) at 0.02 a.u is values for the Map surface are proven in Figure 4 and Fig S3. MEP analysis revealed that the negative potential is concentrated on the N atoms on the imidazole rings (**3a~f, 6a~f**) and oxygen atoms of the NO_2 (3d, 6d) moiety (attached to the benzene ring) and as a result this is the preferred site for electrophilic attack, In addition, the positive charge regions are located on the H atoms on the imidazole (NH group) ring. The negative (-ve) and positive (+ve) potential values of each compound are listed in Table 4.

From the results in Table 4, it is clear that both potential of all testing compounds are seen as about in a similar range and no noteworthy distinction was seen. The minimal value was observed for **6c** (-0.05360 a.u. to 0.05360 a.u), whereas the highest value was observed for **3d** (-0.07353 a.u. to 0.07353 a.u).

3.2. Jack bean urease inhibition study

The current work accounts the study of several chiral benzimidazole derivatives (**3a~f** and **6a~f**) as inhibitors of jack bean ureases. All of the benzimidazoles showed variety of urease inhibitory orders.

As the above experimental values of compounds **3a, 3b** and **3f** revealed that they exhibited good enzyme inhibitory activity with IC_{50} 0.064 and 0.058l M respectively, while benzimidazoles containing no withdrawing groups on benzene ring are quite effective. The compound **3a** (22.26 ± 6.2) acted as good urease inhibitor while the experimental values of **3d** (99 ± 19.4) indicates that the withdrawing moiety (NO_2) on benzimidazole decreases its urease inhibition activity while IC_{50} of reference thiourea is 20.92 M. Another key thing to remember was the structure of acid used in Scheme 1. The smaller acid moiety (Lactic acid) containing benzimidazoles (**3a~f**) were more effective than the one having bulky acid naproxen (**6a~f**).

Imidazole ring has central importance in urease inhibition thus any substitution on side phenyl ring of imidazole can affect the urease

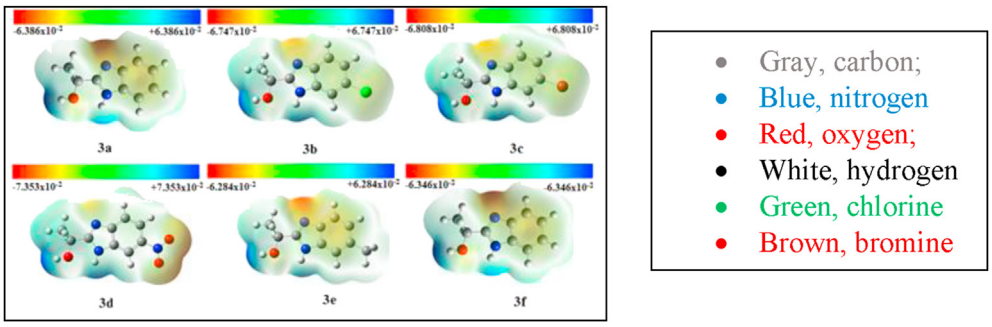

Figure 4. Calculated MEP maps of compounds **3a-f** at B3LYP/6-31G (d,p). (MEP maps of compounds **6a-f** is in figure S3).

Table 4. Values of -ve and +ve potential of products **3a–f, 6a-f** computed at the DFT/B3LYP/6-31G (d,p) level.

Entry	Compound	Negative potential (a.u)	Positive potential (a.u)
1	3a	-0.06386	0.06386
2	3b	-0.06747	0.06747
3	3c	-0.06808	0.06808
4	3d	-0.07353	0.07353
5	3e	-0.06284	0.06284
6	3f	-0.06346	0.06346
7	6a	-0.05524	0.05524
8	6b	-0.05396	0.05396
9	6c	-0.05360	0.05360
10	6d	-0.05997	0.05997
11	6e	-0.05647	0.05647
12	6f	-0.05765	0.05765

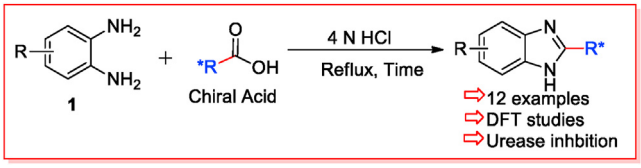

Scheme 1. General scheme for the synthesis of chiral derivatives of benzimidazoles.

inhibition activity of benzimidazole. Based on our research we propose that the chiral benzimidazole 3a, 3b and 3f can serve as good competitive inhibitors.

3.3. Molecular docking studies of chiral benzimidazole with urease enzyme (3LA4)

The compounds **3a** and **6d** along with reference compound thiourea were studied by using docking AutoDock Tools v1.5.6 for protein-

Table 5. Binding affinity of ligands with receptor urease enzyme.

Sr.No.	Ligands	Binding Affinity Kcal/mol
1	**3a** +3LA4	-4.8
2	**6d** +3LA4	-8.6
3	Tiourea+3LA4 (standard)	-3.3

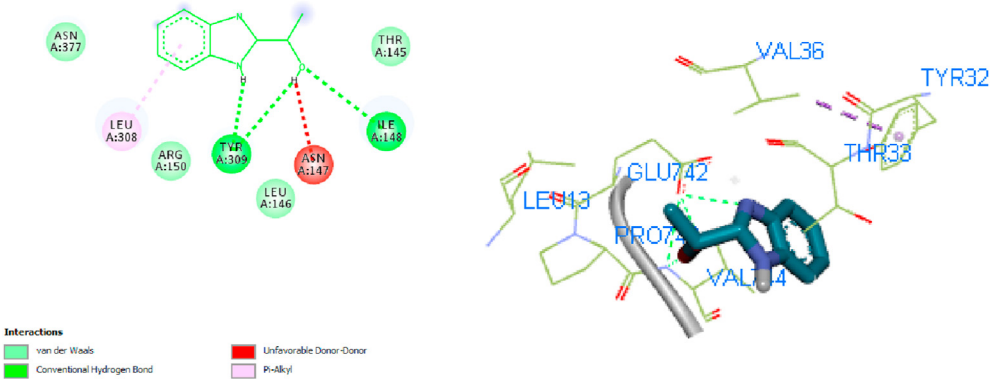

Figure 5. Protein-ligand Interaction between chiral benzimdazole **3a** and active residue of enzyme (3LA4) where Vander Waal forces, hydrogen bonding unfavorable doner-doner and pi alkyl. (Docking for reference thiourea is attached in Figure S9).

ligand docking the virtual screening tool via VINA module. Results are obtained in the form of binding affinity (kcal/mol) which shows the strength of binding interactions between ligand and receptor (Table 5).

As we observed that the order of in-silico and in-vitro results comply with each other. The compound **3a** which is the most potent among our synthesized compounds has shown better binding energy (-4.8 Kcal/mol) as compared to least potent compound **6d** (-8.6 Kcal/mol) (Figure S8). Docking studies revealed that, Hydrogen bond formations were considered as most important for perfect firm fitting of ligand within the active site of enzyme [30]. In the binding model of the most potent compound **3a,** three hydrogen bonds were noticed between residues GLU742, LEU13 and PRO74 with hydroxyl and N–H groups of ligands (Figure 5).

4. Conclusion

Chiral derivatives of benzimidazoles have been synthesized to validate their role in jack bean urease inhibition. All of the above synthesized compounds showed significant inhibition. The compound **3a, 3b** and **3f** were found to be most potent among all above synthesized compounds. Computational studies also enabled us to understand the electronic effects on different substituted chiral benzimidazole. The most responsive sites for nucleophilic and electrophilic attack were predicted by the MEP analysis. On the other hand, FMOs analysis shows that the molecule energy gap for **3a, 3f** is found to be the maximum and equal to 5.61 eV, which influences the biological activity of the compound. While the least band gap (4.48 eV and 3.71 eV,) was determined for **3d, 6d** were not showing significant urease inhibition, because of its low kinetic stability and high chemical reactivity. In addition, docking studies were performed to elaborate the interaction of ligands with residues of active enzyme which was consistent with experimental results. During this study we have found the effect of chirality on urease inhibition whereas the detailed impact of chirality and synthesis of molecules after docking studies is a project underway.

Declarations

Author contribution statement

Naghmana Rashid: Conceived and designed the experiments; Contributed reagents, materials, analysis tools or data.

Hasil Aman: Conceived and designed the experiments; Performed the experiments; Contributed reagents, materials, analysis tools or data; Wrote the paper.

Mohammad Zaman Ashraf: Conceived and designed the experiments; Analyzed and interpreted the data; Wrote the paper.

Nadaraj Sathishkumar: Analyzed and interpreted the data.

Hsin-Tsung Chen: Analyzed and interpreted the data; Wrote the paper.

Aamna Bibi: Contributed reagents, materials, analysis tools or data.

Funding statement

This research did not receive any specific grant from funding agencies in the public, commercial, or not-for-profit sectors.

Competing interest statement

The authors declare no conflict of interest.

Additional information

Supplementary content related to this article has been published online at https://doi.org/10.1016/j.heliyon.2020.e05187.

Acknowledgements

We thank HEJ Karachi for High-Field NMR Center (HFNMRC) and Mass Spectrometry. We are also grateful to the HEC and Alama Iqbal Open University Pakistan for the lab facilities.

References

[1] Y. Bansal, O.M. Silakari, The therapeutic journey of benzimidazoles: a review, Bioorg. Med. Chem. 20 (2012) 6208–6236.

[2] S. Demirci, S. Basoglu, A. Bozdereci, N. Demirbas, Preparation and antimicrobial activity evaluation of some new bi- and tri-heterocyclic azoles, Med. Chem. Res. 22 (2013) 4939–4945.

[3] N. Thamban, K. Sanjib, N. Ranjan, A. Sharma, D.P. Arya, S. Garneau-Tsodikova, New application of neomycin B−Bisbenzimidazole hybrids as antifungal agents, ACS Infect. Dis. 4 (2018) 196–207.

[4] K.S. Eevic, M. Kralj, K. Ester, I. Sabol, M. Grce, K.I. Pavelic, G.K. Zamola, Synthesis, antiviral and antitumor activity of 2-substituted-5-amidino-benzimidazoles, Bioorg. Med. Chem. 15 (2007) 4419–4426.

[5] (a) Y. Ito, K. Shibata, A. Hongo, M. Kinoshita, Ecabetsodium, a locally acting antiulcer drug, inhibitsurease activity of Helicobacter pylori, Eur. J. Pharmacol. 345 (1998) 193–198;
(b) A. Gellis, H. Kovacic, N. Boufatah, P. Vanelle, Synthesis and cytotoxicity evaluation of some benzimidazole-4, 7-diones as bioreductive anticancer agents, Eur. J. Med. Chem. 43 (2008) 1858–1864.

[6] P. Sethi, Y. Bansal, G. Bansal, Synthesis and PASS-assisted evaluation of coumarin–benzimidazole derivatives as potential anti-inflammatory and anthelmintic agents, Med. Chem. Res. 27 (2017) 61.

[7] M. Boiani, M. Gonzalez, Imidazole and benzimidazole derivatives as chemotherapeutic agents, Eur. J. Med. Chem. 5 (2005) 409–424.

[8] X. Jin-Feng, X.L. Jian, ZMo Guang, P.H. Jing, Y.L. Jin, Y.C. Xiao, Y.W. Zhao, Benzimidazole derivatives selective fluorescent chemo-sensors for the pictogram detection of picric acid, J. Org. Chem. 79 (23) (2014) 11619–11630.

[9] A. Atar, Ö. Taspinar, S. Hanft, B. Goldfuss, H.G. Schmalz, A.G. Griesbeck, Hydrogen peroxide sensors based on fluorescence quenching of the 2-aminobenzimidazole fluorophore, J. Org. Chem. 84 (2019) 15972–15977.

[10] R.D. Gautam, Supramolecular synthons in crystal engineering a new organic synthesis, Angewandte chemie Intenational Edition in English 34 (1995) 2311–2327.

[11] (a) H.O. Curkovic, E. Stupnisek-Lisac, H. Takenouti, The influence of pH value on the efficiency of imidazole based corrosion inhibitors of copper, Corrossion Sci. 52 (2010) 398–405;
(b) L.H. Madkour, I.H. Elshamy, Experimental and computational studies on the inhibition performances of benzimidazole and its derivatives for the corrosion of copper in nitric acid, Int. J. Integrated Care 7 (2016) 195–221.

[12] L. Benavent, A. Baeza, M. Freckleton, Chiral 2-aminobenzimidazole as bifunctional catalyst in the asymmetric electrophilic amination of unprotected 3-substituted oxindoles, Molecules 23 (2018) 1374.

[13] (a) F. Arjmand, S. Parveen, M. Afzal, M. Shahid, Synthesis, characterization, biological studies (DNA binding, cleavage, antibacterial and topoisomerase(I) and molecular docking of copper(II)benzimidazole complexes, J. Photochem. 114 (2012) 15–26;
(b) M.L. Lopez-Rodrıguez, B. Benhamu, M.J. Morcillo, I.D. Tejada, L. Orensanz, M.J. Alfaro, M.I. Martın, Benzimidazole derivatives. 2. Synthesis and structure-activity relationships of new azabicyclic benzimidazole-4-carboxylic acid derivatives with affinity for serotoninergic 5-HT3 receptors, J. Med. Chem. 42 (1999) 5020–5028.

[14] M.W. Khalid, H. Ismail, M. Bushra, T. Brendan, A. Zareen, I. Rozas, R.J. Baker, Synthesis, DNA binding and antibacterial activity of metal(II) complexes of a benzimidazole Schiff base, Polyhedron 157 (2019) 326–334.

[15] (a) M. Kot, W. Karcz, W. Zaborska, 5-Hydroxy-1, 4-naphthoquinone (juglone) and 2-hydroxy-1,4-naphthoquinone (lawsone) influence on jack bean ureaseactivity: elucidation of the difference in inhibition activity, Bioorg. Med. Chem. 38 (2010) 132–137;
(b) A. Amtul, A. Rahman, R.A. Siddiqui, M.I. Choudhary, Chemistry and mechanism of urease inhibition, Curr. Med. Chem. 9 (2002) 14;
(c) A. Saeed, S. Mahmood, Z. Ashraf, F. Jabeen, Iminothiazoline-sulfonamide hybrids as jack bean urease inhibitors; synthesis, kinetic mechanism and computational molecular modeling, Chem. Biol. Drug Des. 87 (2016) 434–443.

[16] Luzia V. Modolo, Cristiane J. da-Silva, Débora S. Brandão, Izabel S. Chaves, A mini review on what we have learned about urease inhibitors of agricultural interest since mid-2000s, J. Adv. Res. 13 (2018) 29–37.

[17] (a) J.J. Sigurdarson, S. Svane, H. Karring, The molecular processes of urea hydrolysis in relation to ammonia emissions from agriculture, Rev. Environ. Sci. Biotechnol./Technol. 17 (2018) 241–258;
(b) J. Zhang, Z. Wang, C. He, X. Liu, W. Zhao, S. Sun, C. Zhao, Safe and effective removal of urea by urease-immobilized, carboxyl-functionalized PES beads with good reusability and storage stability, ACS Omega 4 (2019) 2853–2862.

[18] J. Prywer, M. Olszynski, E.M. Brzoska, Green tea and struvite crystals in relation to infectious urinary stones: the role of (−)-Epicatechin, Cryst. Growth Des. 17 (2017) 5953–5964.

[19] (a) C.A. Francis, K.J. Roberts, J.M. Beman, A.E. Santoro, B.B. Oakley, Ubiquity and diversity of ammonia-oxidizing archaea in water columns and sediments of the ocean, in: Proceedings of the Natural Academy of Sciences, 2005, pp. 14683–14688;

(b) M. Zaman, M.L. Nguyen, J.D. Blennerhassett, B.F. Quin, Reducing NH_3, N_2O and NO_3 losses from a pasture soil with urease or nitrification inhibitors and elemental S-amended nitrogenous fertilizers, Biol. Fertil. Soils 44 (2008) 693–705.

[20] L. Mazzei, M. Cianci, S. Benini, S. Ciurli, The structure of the elusive urease–urea complex unveils the mechanism of a paradigmatic nickel-dependent enzyme, Angew. Chem. Int. Ed. 58 (2019) 7415–7419.

[21] P. Kafarski, Michał Talma, Recent advances in design of new urease inhibitors: a review, J. Adv. Res. 13 (2018) 101–112.

[22] A.G.M. Al-Sehemi, A. El-Sharief, Y.A. Ammar, Propionic acids in organic synthesis: novel synthesis of benzimidazole, 3,1-benzoxazine, 3-aminoquinazoline and 3-aminothieno[2,3-d]pyrimidine derivatives containing 2-naphthyl propionyl moiety, Indian J. Chem. 45 (2006) 450–455.

[23] Y. Wang, K.T. Tai, J.H. Yen, Separation, bioactivity, and dissipation of enantiomers of the organophosphorus insecticide fenamiphos, Ecotoxicol. Environ. Saf. 57 (2004) 346–353.

[24] A. Saeed, S. Mahmood, M. Rafiq, Z. Ashraf, F. Jabeen, S.Y. Seo, Iminothiazoline-sulfonamide hybrids as jack bean urease inhibitors; synthesis, kinetic mechanism and computational molecular modeling, Chem. Biol. Drug De 87 (2016) 434–443.

[25] (a) V.V. Menon, E. Foto, Y. Mary S, E. Karatas, C.Y. Panicker, G. Yalcin, S. Armakovi, J. Sanja, C. Armakovi, V. Alsenoy, V.I. Yildiz, Vibrational spectroscopic analysis, molecular dynamics simulations and molecular docking study of 5-nitro-2-phenoxymethyl benzimidazole, J. Mol. Struct. 1129 (2017) 86–97;
(b) L.M. Dudd, E.V. Venardou, E. Garcia-Verdugo, P. Licence, A.J. Blake, C. Wilson, M. Poliakoff, Synthesis of benzimidazole in high temperature water, Green Chem. 5 (2003) 187–192;
(c) A. Pandey, H. Mohammed, K.A. Anil, Chiral benzimidazole-derived mono aza-crowns: synthesis and enantiomer recognition studies with chiral amines and their ammonium salts, Tetrahedron-Asymmeter 24 (2013) 706–712.

[26] (a) S. Das, S. Mallick, S.D. Sarka, Cobalt-catalyzed sustainable synthesis of benzimidazoles by redox-economical coupling of o-nitroanilines and alcohols, J. Org. Chem. 84 (2019) 12111–12119;
(b) D.Y. Kim, P.D.Q. Dao, C.S. Cho, Synthesis of pyrimidine- and quinazoline-fused benzimidazole-4,7- diones using combinatorial cyclocondensation and oxidation, ACS Omega 3 (2018) 17456–17465;
(c) Murat Beytur, Zeynep Turhan Irak, Sevda Manap, Haydar Yüksek, Synthesis, characterization and theoretical determination of corrosion inhibitor activities of some new 4,5-dihydro-1H-1,2,4-Triazol-5-one derivatives, Heliyon 5 (2019), e01809.

[27] (a) S. Singhal, P. Khanna, L. Khanna, Synthesis, DFT studies, molecular docking, antimicrobial screening and UV fluorescence studies on ct-DNA for novel Schiff bases of 2-(1-aminobenzyl) benzimidazole, Heliyon 5 (2019), e02596;
(b) M. Alam, D.U. Lee, Synthesis, spectroscopic and computational studies of 2-(thiophen-2- yl)-2,3-dihydro-1H-perimidine: an enzymes inhibition study, Comput. Biol. Chem. 64 (2016) 185–201;
(c) Y.S. Mary, Y.S. Mary, K.S. Resmi, R. Thomas, DFT and molecular docking investigations of oxicam derivatives, Heliyon 5 (2019), e02175.

[28] (a) M. Frisch, G.W. Trucks, H.B. Schlegel, G.E. Scuseria, M.A. Robb, J.R. Cheeseman, G. Scalmani, V. Barone, B. Mennucci, G.e. Petersson, Gaussian~ 09 Revision D. 01, 2014;
(b) A. Singh, H. Singh, J.M. Khuranaa, Computational study of new 1,2,3-triazole derivative of lithocholic acid: structural aspects, non-linear optical properties and molecular docking studies as potential PTP 1B enzyme inhibitor, Comput. Biol. Chem. 78 (2019) 144–152;
(c) M. Alama, M.J. Alam, A. Shaista, M. Parveen, S. Park, S. Ahmad, DFT/TD-DFT calculations, spectroscopic characterizations (FTIR, NMR, UV–vis), molecular docking and enzyme inhibition study of 7-benzoyloxycoumarin, Comput. Biol. Chem. 73 (2018) 65–78.

[29] J.M. Roque, T. Pandiyan, J. Cruz, E. García-Ochoa, DFT and electrochemical studies of tris(benzimidazole-2-ylmethyl)amine as an efficient corrosion inhibitor for carbon steel surface, Corrosion Sci. 50 (2008) 614–624.

[30] E. Menteşe, M. Emirik, B.B. Sökmen, Design, molecular docking and synthesis of novel 5,6-dichloro-2-methyl-1Hbenzimidazole derivatives as potential urease enzyme inhibitors, *B*ioorg. Chem. **86** (2019) 151–158.